

Original Study

Open Access

Katarzyna Gabryś\*, Katarzyna Markowska-Lech\*, Wojciech Sas

# Small-strain stiffness of selected anthropogenic aggregates from bender element tests

<https://doi.org/10.2478/sgem-2024-0013>

received March 18, 2024; accepted May 14, 2024.

**Abstract:** This article presents a study on the stiffness of mixtures of anthropogenic materials derived from construction or demolition waste, specifically fine recycled concrete aggregates (fRCAs) with different fine fraction (FF) contents. The study investigated small-strain shear moduli via various signal interpretation methods, examining, above all, the time domain approaches and considering the influence of FF content. However, the inconclusive results from the bender element (BE) tests highlight the complexity of factors affecting shear wave velocity, which requires further research to refine the methodology and assess long-term performance in geotechnical applications.

Selecting the correct test frequency and interpretation method is crucial to obtain accurate results. The BE test method should consider all relevant factors. At low input frequencies ( $\leq 5$  kHz), the near-field effect affected the received signal for fRCA mixtures. At higher frequencies (around 14 kHz), the noise levels increased, thereby interfering with the S-wave travel time determination. Intermediate input frequencies (10.0 and 12.5 kHz) provided the representative shear modulus ( $G$ ) values. The small-strain shear modulus ( $G_{\max}$ ) of the fRCA compounds from the resonant column and BE tests was found to be in good agreement, despite differences in the test procedures themselves.

**Keywords:** piezoelectric transducers; initial shear modulus; recycled material; travel time interpretation.

## 1 Introduction

Increasing economic activities in developing countries result in more energy and consumption demand, which generally leads to environmental degradation. As environmental awareness has grown, the idea of sustainable development has become widespread. The concept of sustainable development can be broadly defined as an attempt to reconcile growing environmental and social concerns (Hopwood et al., 2005). To preserve the ecological balance, it is very important to meet people's socioeconomic needs. Sustainability plays a crucial role in geotechnical engineering. To be sustainable, an engineering system should be effective, dependable, robust, and adaptable. Efficiency means minimizing the engineered system's resource use, cost, and environmental impact. As an important part of the construction industry, geotechnical engineering has the potential to have a major impact on sustainable development. Geotechnical works can be responsible for large movements of soil, associated energy consumption, and significant use of natural and man-made materials. Geotechnical engineers have a major impact on the natural environment and water resources by modifying the earth's surface, altering soil properties, and dealing with contamination. They are often involved in the selection of sites for major infrastructure works, transport services, and buildings, which can have a significant impact on the social and economic aspects of the project (Basu et al., 2013).

Recent research studies on geosustainability are mostly based on the common notions of sustainability, such as recycling, reuse, and use of alternate materials, technologies, and resources. One of the areas in which geotechnical research is making great strides is the use of alternative, environmentally friendly materials in geotechnical construction and the reuse of waste materials (Jastrzębska and Łupieżowiec, 2023). Such materials are, for example, recycled aggregates, that is, reprocessed aggregates derived from demolition or construction waste that contribute to a circular economy by repurposing reclaimed material and waste. Recycled concrete aggregate (RCA) is a promising economic

\*Corresponding author: Katarzyna Gabryś, Katarzyna Markowska-Lech, Department of Geotechnical Engineering, Institute of Civil Engineering, Warsaw University of Life Sciences - SGGW, 159 Nowoursynowska Street, 02-776 Warsaw, E-mails: katarzyna\_markowska-lech@sggw.edu.pl; wojciech\_sas@sggw.edu.pl  
**Wojciech Sas**, Department of Geotechnical Engineering, Institute of Civil Engineering, Warsaw University of Life Sciences - SGGW, 159 Nowoursynowska Street, 02-776 Warsaw

and environmental substitution for natural aggregates (Gabryś et al., 2023a). European countries have been seeking to employ RCA in new concrete structures since the early 1980s (Behera et al., 2014). More than 40 years ago, research began on the characteristics of RCA. RCA manufacturing provides sustainability for concrete waste and encourages recycling rather than landfill. In addition, it focuses on the lack of natural aggregates, minimizes the need for them, and ultimately allows the preservation of the natural course aggregates mined in the open pit. Despite the cost, these and many other benefits have led to an increase in interest in the production and use of RCA in design (Makul et. al., 2021).

In modeling the behavior of RCA when used as a geotechnical material, stiffness at small strains is a key property. Material small-strain stiffness is a critical parameter for predicting deformations of geostructures and soil–structure interaction problems. The stiffness of geomaterials, including the shear modulus ( $G$ ), modulus of rigidity ( $M$ ), and elastic modulus ( $E$ ), has its maximum value in the elastic regime (generally less than 10<sup>-3</sup>% strain). The bender element (BE) test (Shirley and Anderson, 1975), a high-frequency dynamic testing technique that uses a pair of techniques using a pair of piezoelectric element inserts, is widely adopted to record the shear wave velocity ( $V_s$ ) to derive the small-strain soil shear modulus ( $G_{max}$ ) (Viggiani and Atkinson, 1995; Jovicic et al., 1996; Youn et al., 2008). A BE test is a relatively simple nondestructive test for measuring shear and compression wave velocities and determining shear modulus. However, different factors that affect the measurement of the travel time in the BE tests cause difficulties in the selection of a reliable method to determine the first arrival time, and there is no standard procedure for these experiments (Markowska-Lech et al., 2018).

Piezoelectric transducer applications for natural soils were originally introduced by Lawrence in the 60s (1963), and from then on, the experimental setting as well as the methods of signal interpretation (e.g., Wang et al., 2017) have improved. Some attempts to apply the BE technique to study the stiffness of recycled materials have been recently made. In particular, the authors studied the shear wave velocity in the time and frequency domains (TD and FD, respectively) of pure coarse concrete aggregate from concrete curbs from the demolition of roads and its modified versions, that is, mixtures with 15% rubber chips by RCA volume (Gabryś et al., 2017). The results showed that tire chips significantly decrease the  $V_s$  values of the modified RCA. They helped to reduce the near-field effect, but the received parameters were more incoherent. The  $V_s$  values were found to be influenced by the interpretation

technique, mean effective stress, and wave propagation period. The maximum  $V_s$  values were obtained mostly from the FD method, although TD analysis gives more coherent results.

The current study examined the small-strain shear moduli of compacted, saturated, and isotopically consolidated mixtures of anthropogenic materials. Here, fine recycled concrete aggregates (fRCAs) with varying fine fraction (FF) contents ( $0\% \leq FF \leq 30\%$ , within increments of 5%) were selected as the test material. During evaluation of the use of the  $G_{max}$  modulus as a crucial indicator to monitor response development, the need for proper interpretation of the transmitted signal arose. Therefore, different methods of interpretation and different excitation frequencies were applied, with the additional purpose of highlighting how fine content can affect BE testing. In addition, a comparison of the test results obtained from the BE method with those from the standard resonant column (RC) tests is provided.

## 2 Methodology

### 2.1 BE Test

BEs comprise two thin piezoceramic plates that are rigidly attached to a central metal plate. Due to the properties of the piezoceramic material, when excited by an input voltage, one piezoceramic plate stretches and the other shortens. This acts like

a transmitter, producing a mechanical stimulus. When a bending element is mechanically excited, it produces an electrical output and acts as a signal receiver. From the theory of wave propagation, and assuming that the mass of soil is semi-infinite, homogeneous, and elastic, the modulus of elasticity in small strains can be calculated from the following equation (1):

$$G_{max} = \rho \cdot V_s^2 \quad (1)$$

where  $\rho$  is the bulk density of soil and  $V_s$  is the shear wave velocity (Viggiani, 1995, Brignoli et al., 1996, Kawaguchi et al., 2001).

To determine  $V_s$  using the BE technique, two measurements are required: i) the travel distance ( $L_t$ ) and ii) the travel time ( $t$ ). The shear wave velocity can be calculated by equation (2) (Brignoli, et al., 1996):

$$V_s = L_t/t \quad (2)$$

The  $L_{tt}$  parameter is easy to measure as it is defined as the distance between the ends of BEs. A more challenging aspect is to identify the travel time. So far, various methods have been tested to determine the wave propagation time. The methodologies for estimating the travel time of the shear wave are classified broadly into two groups: TD- and FD-based approaches. At present, however, neither is universally accepted as a perfect technique for estimating the appropriate travel time for any soil or test condition.

The TD-based approach involves the problem of the “near-field effect,” which often results in significant errors in travel time measurement because of the bias in the early part of the output signal. Since there is still some uncertainty about how much the near-field effect will distort the output signal in a given state, the experimenter is forced to rely on trial and error to arrive at an appropriate delay. Meanwhile, the FD-based approach has the advantage of minimizing human error when measuring. However, it has been found that the resulting travel times are, in general, highly scattered and are smaller than those obtained by the TD approach. Thus, the difficulty in estimating the appropriate travel time remains. The meaning of the resulting output signal is not understood well enough theoretically to solve the problem (Ogino, 2019).

## 2.2 Materials and Test Methods

The laboratory tests presented in this paper were carried out in the GDS Instruments (a division of Global Digital Systems Ltd) GDS RC apparatus on the compounds of crushed concrete waste originating from a demolition site in Warsaw, Poland. The test material was provided by the capital’s supplier, directly in a shredded form. The recycled concrete delivered consisted of well-graded aggregate, which included gravel, sand, and silt-sized grains. Therefore, further crushing of the coarser gravel fraction as well as sieving were conducted before testing, and sand-sized or sand with soil-sized aggregates was the focus of this study. Six different compositions with the specimen codes M1, M2, M3, M4, M5, and M6 were studied and the details of these compositions are given below:

- M1, M2, M3, M4 – a group of mixtures in air-dry conditions, with a grain size of 0/2 and an FF content of RCA of 0%, 10%, 20%, and 30%, respectively;
- M5, and M6 – a group of moisturized mixtures with a grain size of 0/2 and an FF content of RCA of 5% and 15%, respectively.

The grading curves for all the materials are given in Fig. 1, together with an image of the parent concrete aggregate. Table 1 gives a summary of the physical properties of the tested RCA. Based on the physical characteristics and the particle size distribution curves, the blends were classified as poorly graded fine SANDS (M1, M2, and M5 blends) ( $FF \leq 10\%$ ), poorly graded SANDS with silt (M6 blend) ( $FF = 15\%$ ), and well-graded SANDS with silt ( $FF > 15\%$ ) according to the unified soil classification system specified in, for example, PN-EN ISO 14688-2:2018-05. The samples were produced by evenly mixing two materials, that is, pure fRCA and the calculated amount of FF for this fRCA. A detailed description of the mixes’ preparation and a report from other tests carried out on this material can be found in Gabryś et al. (2023b).

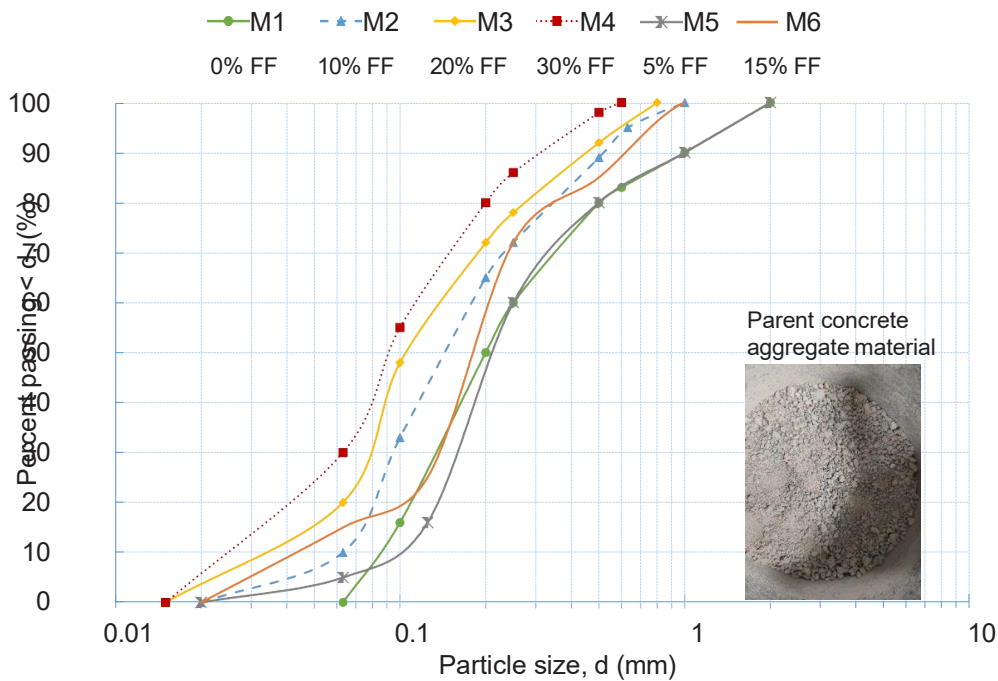
The GDS RC apparatus, an example of the fixed-free type of Stokoe RC system with BE inserts implemented, was used in the present study. A schematic of the testing system is available in many publications like He et al. (2018) and Gabryś et al. (2023b). The RC system adopted by the authors houses a specimen with dimensions of 14 cm in height and 7 cm in diameter. A range of isotropic pressures from 90 to 270 kPa was applied to each specimen. Both the top cap and the base were fitted with piezo-inserts. They protrude 3 mm out of the platen. The width and thickness of BEs are 11 and 1 mm, respectively. The BE test setup is shown in Fig. 2. When

configured to the BE mode, one of the piezo-inserts triggers shear waves (S-waves) and the other acts as a receiver (Fig. 3), while in the extender element (EE) mode, the roles of sender and receiver are exchanged to generate and receive primary waves (P-waves) (Lings and Greening, 2001).

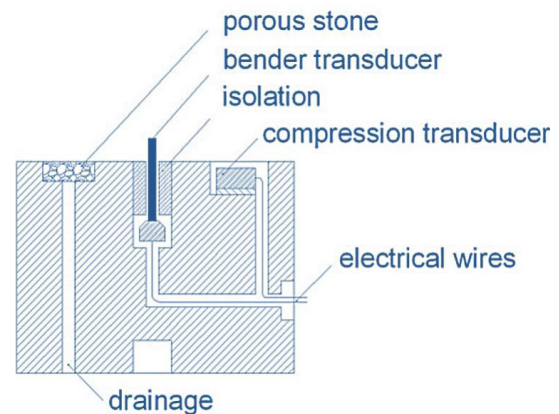
Compacted specimens were prepared in a two-piece metal split mold of four layers of similar heights from the oven-dried RCA. For the last two mixtures, that is, M5 and M6, RCA was moistened to a value close to the optimum moisture content (OMC). OMCs were set at 13.5% and 16% for the M5 and M6 mixes, respectively (Gabryś et al., 2023b). To compact the specimens, a lightweight rod was used, targeting a relative density ( $D_r$ ) of more than 65%. Before removal of the mold, a small vacuum (~5–10 kPa) was applied to hold the specimen. Its dimensions were then measured and recorded to calculate the initial void ratio ( $e_0$ ) (Table 1). All the mixtures were consolidated isotropically in progressive stages. The BE tests were conducted at three different pressures, that is, 90, 180, and 270 kPa, after each stage of consolidation had been completed. Such values cover typical stress levels encountered in practice in many geotechnical applications of anthropogenic materials (Tasalloti et al.,

**Table 1:** Fundamental physical properties of RCA in this work.

No.	Specimen code	Fraction (mm)	Mean grain size $D_{50}$ (mm)	Specific gravity $G_s$	Preparation method	Initial void ratio $e_0$	Initial dry unit weight $\gamma_{d,0}$ (kN/m <sup>3</sup> )
1	M1	0.063–2.0	0.2	2.61	Dry tamping	0.61	16.29
2	M2	0.02–1.0	0.16	2.61	Dry tamping	0.63	16.08
3	M3	0.015–0.8	0.14	2.61	Dry tamping	0.72	15.43
4	M4	0.015–0.6	0.21	2.61	Dry tamping	0.81	14.62
5	M5	0.02–2.0	0.21	2.61	Moist tamping	0.74	14.96
6	M6	0.02–1.0	0.18	2.61	Moist tamping	0.71	15.00

**Figure 1:** Grading curves of RCA specimens tested; image of the parent RCA.

2020). The input signal, a sine pulse of 14 V amplitude, was generated by a function generator. Sine-wave pulses have become more popular within different input wave shapes, as these have been shown to give more reliable time measurements primarily (Blewett et al., 2000). The magnitude of the input signal was selected at 14 V as the typical one preferred when using the GDS BE system. Several frequencies were applied, ranging from 3.3 to 25.0 kHz, depending on the mixture and the effective stress. The frequency range is limited by a value of 25.0 kHz due to the characteristics of the transducers, filters, and amplifiers and the resolution of the acquisition system.

**Figure 2:** Schematic drawing of the triaxial base with bender element configuration (after Brignoli et al., 1996).

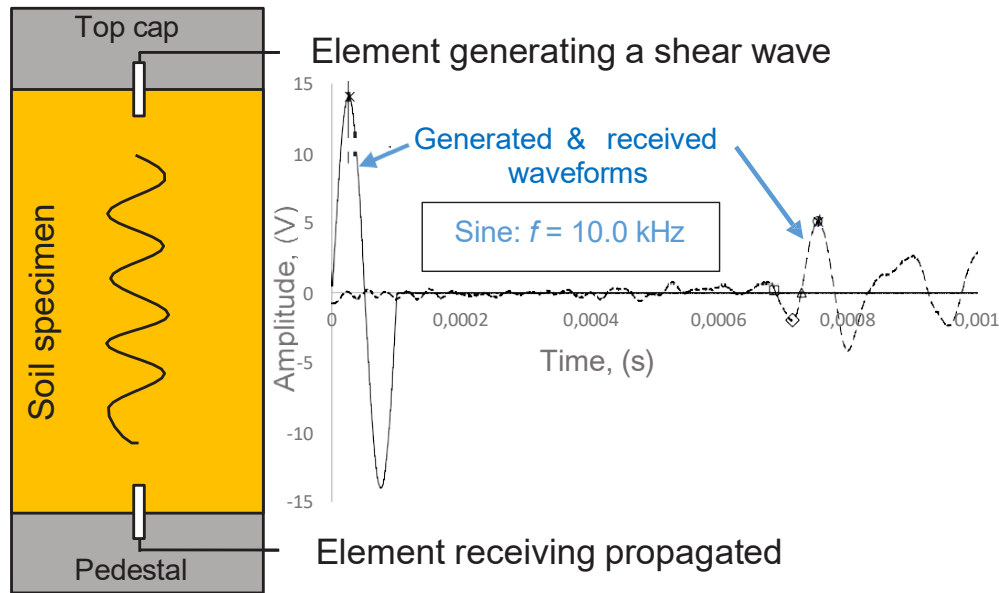


Figure 3: Schematic illustration of an S-wave bender element test, displaying generated and received waveforms.

## 3 Results and Discussion

### 3.1 Selected Factors Influencing Waveform Reading

The appeal of the BE technique lies in its apparent simplicity, both in performing the test and in interpreting the results. However, over the years, several researchers have demonstrated several potential (inherent and induced) sources of error involved in both BE testing and interpretation. Among these, the most common are near-field effects, wave interferences at the rigid boundaries, specimen geometry, transducer resonance, overshooting, electric noise, and grounding/shielding issues (Viana da Fonseca et al., 2009).

To avoid some of these errors, it is first recommended to comply with several technical requirements and boundary conditions (Lee and Santamarina, 2005). These include properly shielded and grounded, properly connected and encapsulated sensors, leakproof connections, and an environment free of noise. There are also other aspects involved, particularly spatial factors, including the orientation of BE, the wave being reflected off the edges and sides of the sample, and the relative distance between the transmitter and the receiver. Poor contact between BE and the soil, leading to poor coupling, especially at low confining pressures, and overshoot, as BE changes its dominant mode shape at high frequencies and the response becomes complex, are further issues that require consideration.

The input excitation frequency may greatly affect the results of BE tests because of the near-field effects and noise. The near-field component of the wave causes the transmitted wave to be distorted at its origin point, and the wave starts with a downward or upward deflection as described and presented in Ingale et al. (2017). As the shear wave propagates, two different wave signals are produced. One component of this signal wave propagates in the longitudinal direction and the other component propagates as a shear wave, which makes it difficult to distinguish the S-wave propagation time due to the early arrival of the P-wave component. This effect is more prominent when the transmitter and the receiver come closer. To minimize the near-field effect, some authors have suggested using higher input frequencies and wavelength ratios (Wang et al., 2007). The wavelength ratio ( $R_d$ ) is defined according to equation (3) (Scarrow and Gosling, 1986) as follows:

$$R_d = L_{tt}/\lambda = (L_{tt}/V_s) \cdot f_{in} \quad (3)$$

where  $f_{in}$  is the excitation frequency and  $\lambda$  is the wavelength of input signals. As widely reported in the literature (e.g., Arroyo et al., 2003; Arulnathan et al., 1998), the wavelength ratio values  $R_d < 2$  or  $> 9$  are associated with prevailing near-field effect, which masks the actual arrival of the received signal that is consequently difficult to be read. According to Sanchez-Salinero et al. (1986), to completely separate the P- and S-wave signals, the  $R_d$  values must be greater than 4.



The graphical representation of the test results for the M1 and M4 blend and all applied input signal frequencies for this mix is presented in Fig. 4a and b. Similar plots can be obtained for all other mixtures and pressures. The wavelength ratio ( $R_d$ ) for the M1 mixture varies between 2.6 and 11.6 for frequencies between 3.8 and 16.7 kHz, whereas for the M4 mixture,  $R_d$  falls between 1.7 and 11.0 for  $f_{in}$  from 3.8 to 16.7 kHz. From the data shown in Fig. 4, it is observed that irrespective of the specimen tested, at low frequencies (i.e., 3.3–5 kHz), the wavelength ratio for the studied RCA is lower than 4, which is required to avoid near-field effects in the case of sand or sand with silt (e.g., Zhou et al., 2010; Juneja and Endait, 2013). It should be recalled here that the mixtures tested were classified as sands and sands with silt in terms of grain size distribution. It is also worth noticing that the received signal, where the  $R_d$  ratio is less than 2 (Fig. 4b), has no obvious peak due to the near-field effect. There are other factors as well that affect the correct interpretation of the signal at lower frequencies, like wave attenuation. At a higher  $R_d$  ratio, however, the noise level appears to increase causing some problems in S-wave travel time determination. This is primarily because a high-frequency signal is more prone to attenuation or interference during propagation, suggesting sensitivity of the signal quality toward  $L_r/\lambda$ .

The latest research on natural soils and their compounds indicates that an excitation frequency of the input signal ( $f_{in}$ ) close to the resonant frequency ( $f_r$ ) can produce a very clear received waveform (Viana da Fonseca et al., 2009). As reported in the resonance tests of RCA tested in the current study and described as well in a previous study by Gabryś et al. (2023b), the estimated  $f_r$  values were lower than 1 kHz for all the RCA mixtures and all the effective stresses. These resonant frequencies were obtained for the full system under continuous signals (steady state). Unlike the natural soils, the criterion for the selection of the best excitation frequency in BE tests near the resonant frequency is not satisfied regarding the RCA used. Hence, the reading of the actual arrival time of the received signal is very difficult here for  $f_{in} = f_r$ .

Fig. 4a indicates that at  $p' = 90$  kPa, determination of the travel time is quite straightforward; however, Fig. 4b shows that at higher stresses ( $p' = 270$  kPa), interpretation is ambiguous. Similar observations were recorded for natural soils, residual soil from Porto granite, and Toyoura sand in studies by Viana da Fonseca et al. (2009).

In Fig. 5, the small-strain modulus  $G_{max}$  at different wavelength ratios for the M4 mixture, as an example, is illustrated. The  $G_{max}$  values were calculated through the peak-to-peak method. In this graph, the previously

mentioned limits for the  $R_d$  values are marked. In this way, a certain narrow range of frequencies (between 5 and 14 kHz for  $p' = 90$  kPa, and up to 20 kHz for  $p' = 180$  and 270 kPa) was created. It may be a great suggestion if the BE tests are performed on the RCA mixtures to obtain clearer waveforms. It is shown that in this defined frequency range, the  $G_{max}$  modulus has a slight upward trend. The average value of  $1/G_{max}$  was a maximum of 4%. Compared to the tests performed on natural soils (Wang et al., 2021), there are no stable values of the small-strain shear modulus as the  $R_d$  or excitation frequency increases. Most likely, the reason for this is the self-compaction with simultaneous crushing of the concrete aggregates with increasing frequency excitation. Due to the very irregular shape of crushed concrete grains, the crushing effect is observed even in the case of dynamic tests. The phenomenon of breakage of the RCA grains was described in detail by He and Senetakis (2016), who revealed that breakage of the RCA grains for samples subjected to pressures even smaller than 1 MPa was greater than the corresponding breakage in sands.

### 3.2 Selected Signal Interpretation Methods

Various methods have been proposed over the years for interpreting the received signals, ranging from the simplest, based on direct observation of the waveforms and measurement of the time interval between the starting points, to more sophisticated techniques supported by signal processing and spectrum analysis tools. Both TD and FD methods were initially taken into account for signal interpretation in BE testing of RCA. A short description of the main principles and applications of each method is given.

The first group of methods is based on the observation of the transmitted and received wave signals and the calculation of their difference as the travel time in the soil sample. With this technique, the arrival time of the shear wave is affected by the near field, the influence of compression wave signals, and other electrical noise and reflections. As a result, it is often difficult to read the arrival time (Sas et al., 2016). Viggiani and Atkinson (1995) compared the initial arrival of the received signal at different possible locations. Fig. 6 gives an example of different potential points of the resulting output signal. Point A is the first deflection; point B is the first inflection (first peak; point maximum); point C is the first zero after the inflection (zero crossing); and point D is the second inflection. Characteristic points of the input and output waves, such as peaks, troughs, and zero

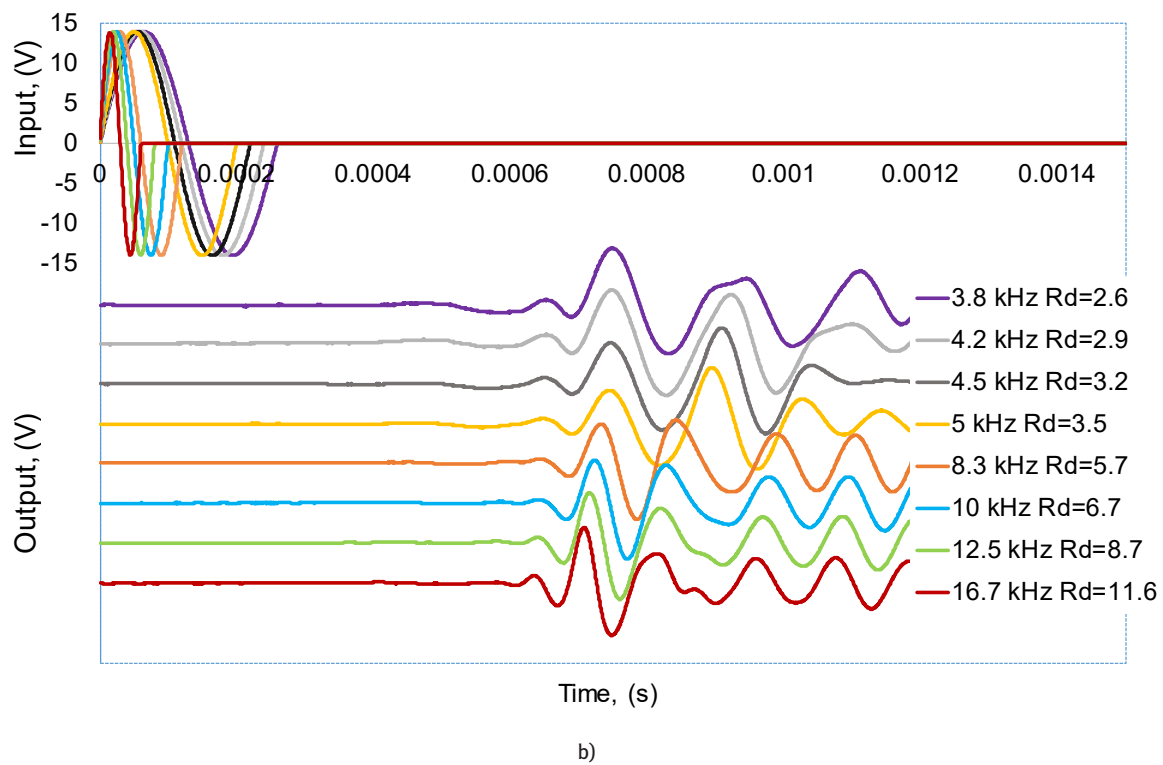
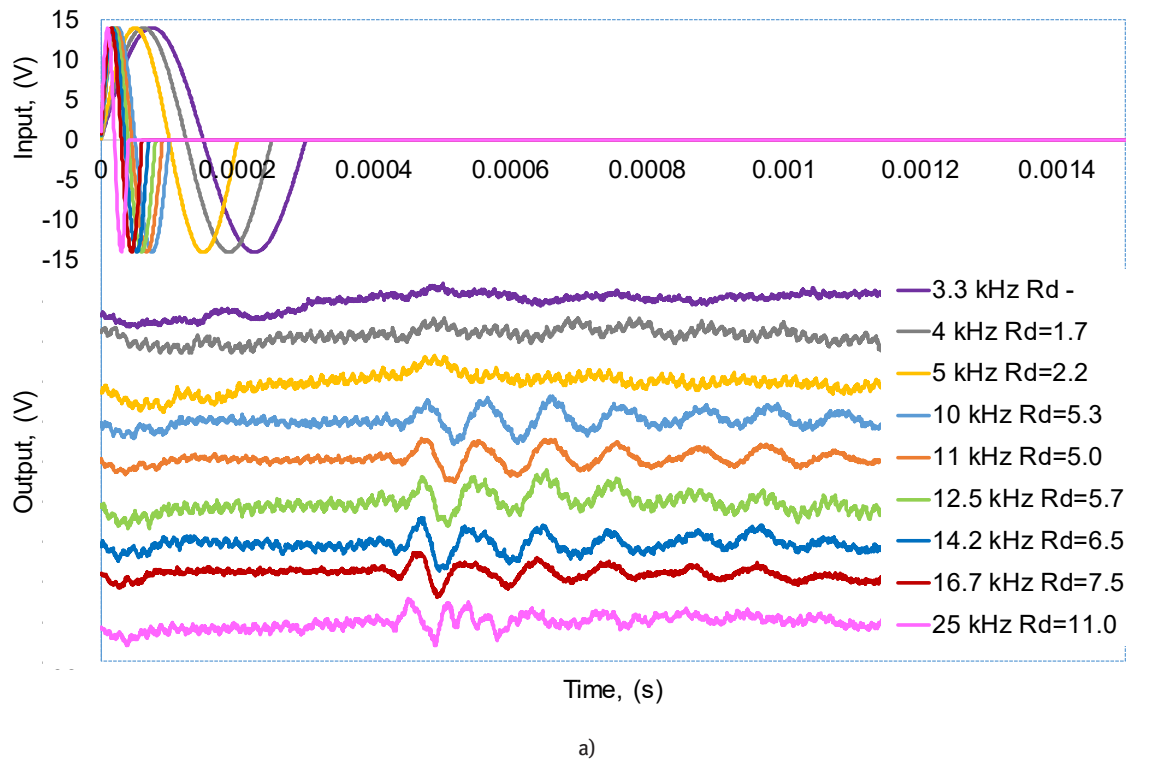


**Figure 4:** Example input and received signals in bender element tests; waveform and wavelength ratio at different frequencies for a) the M1 mixture ( $p' = 90$  kPa) and b) the M4 mixture ( $p' = 270$  kPa).

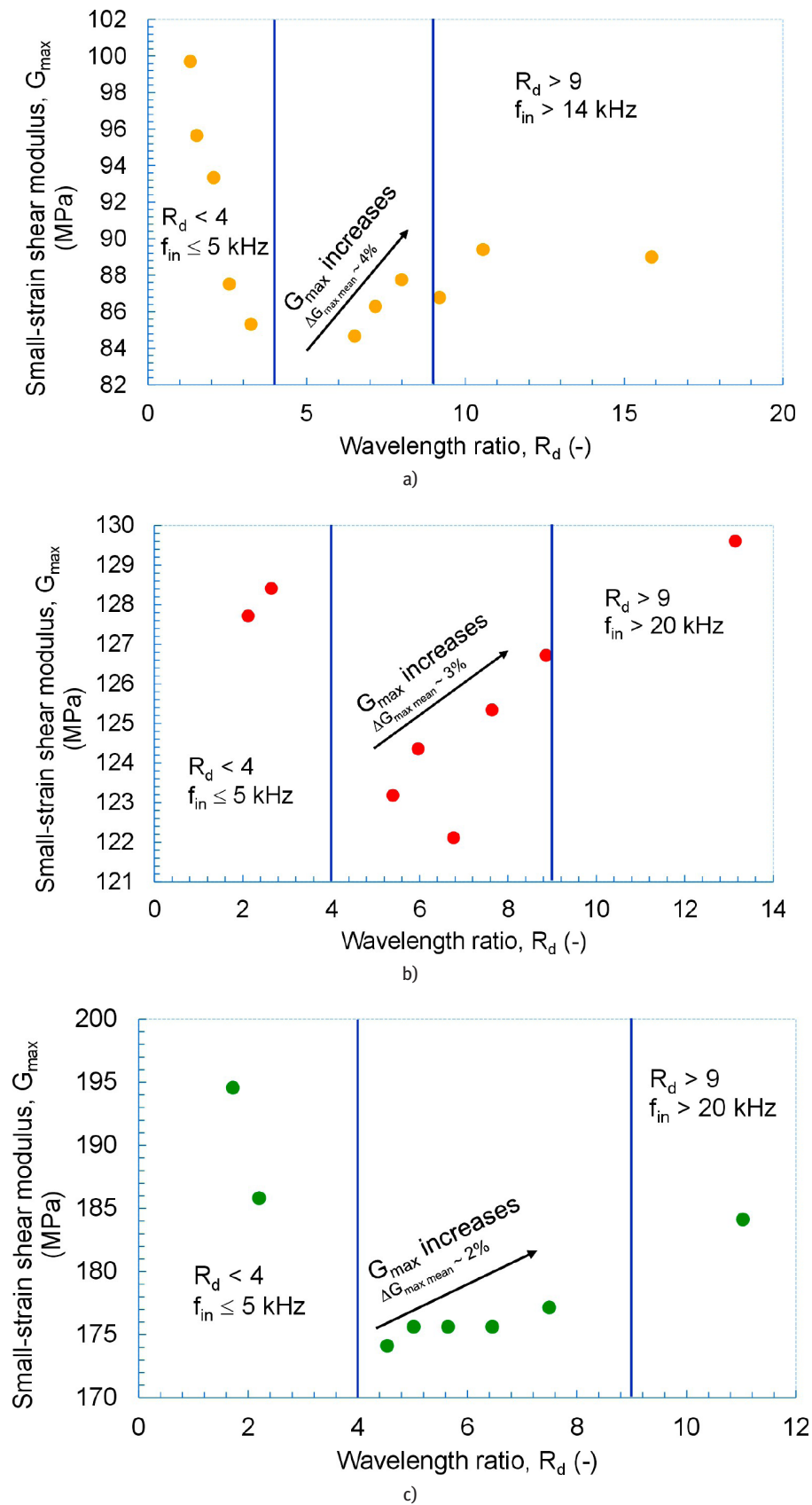


**Figure 5:** Example  $G_{\max}$  values determined for the M4 mixture versus the wavelength ratio at a)  $p' = 90$  kPa, b)  $p' = 180$  kPa, and c)  $p' = 270$  kPa.



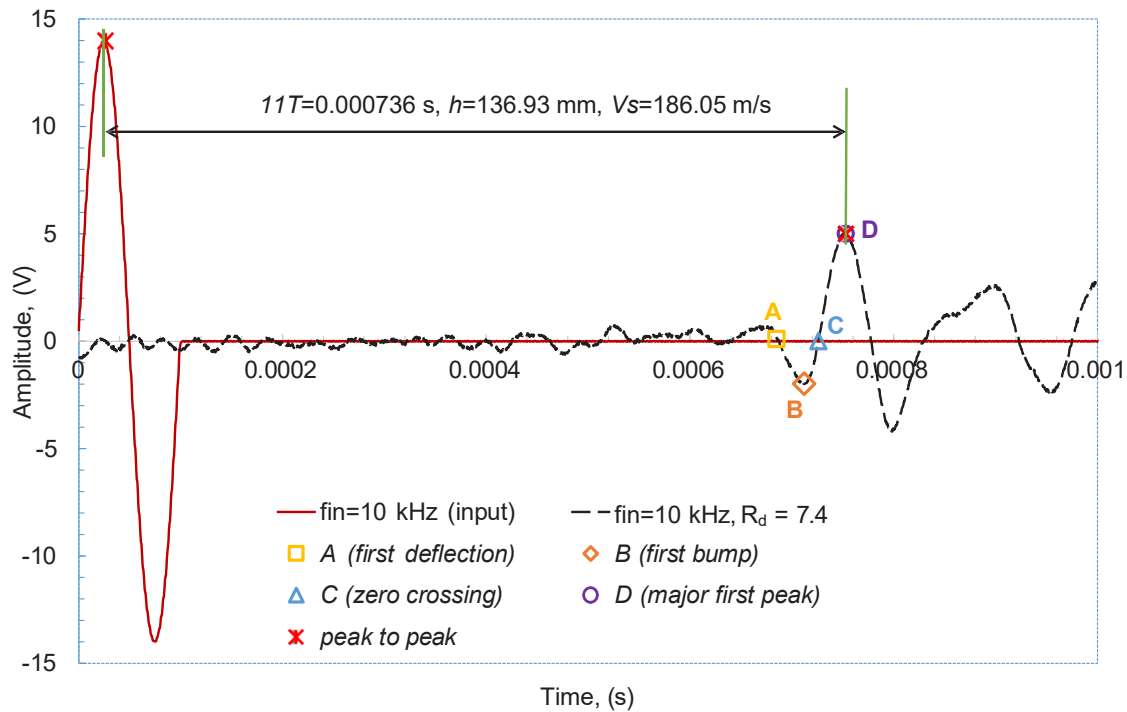


Figure 6: Example of potential arrival points (the M1 mixture,  $p' = 90$  kPa).

intercepts, are easy to identify, and the intervals between the corresponding points can be considered to represent the travel time of the S-wave, again under the assumption of plane wave propagation and absence of reflections or refractions (Viggiani and Atkinson, 1995). 15

Based on the same assumptions as above, Viggiani and Atkinson (1995) suggested using a cross-correlation (CC) function, which measures how two signals are correlated. CC of a low-frequency impulse and the response produce a time displacement, which can be used as the time of flight of the wave between the two points (Mohsin and Airey, 2003). Such a technique is strictly applicable to signals of the same amplitude, requiring frequencies of both waves of the same magnitude (Santamarina and Fam, 1997). However, it is not clear what, if any, benefit is there in using CC to match a single-pulse input signal and a more complex output signal.

The second group of methods calculates the cross spectrum of the transmitted and the received waves, producing the relations of the amplitude and phase angle with the frequency axis. The arrival time is then computed from the phase spectrum slope. As the frequency characteristics of the input and output waveforms are used, this is sometimes called the FD method (Yamashita et al., 2007).

Both groups of procedures require an experienced researcher with a proper knowledge of how to interpret

the correlated result. There is also a subjective aspect to this testing technique.

Moreover, the same method used by the same researcher on the same test apparatus can provide different levels of interpretation reliability, simply because of the different properties of the soil. In the subsequent section of the article, only travel time interpretation issues for the RCA specimens will be examined.

In Fig. 7, the results of the small-strain shear modulus ( $G_{\max}$ ) from the BE test using different analysis methods versus the mean effective stress ( $p'$ ) from one representative specimen, the pure fRCA (the M1 blend) with FF = 0%, are illustrated. The arrival points A, B, C, D, and peak to peak 2 method were read automatically in the GDS BEAT program (Multi-Method Automated Tool for Travel Time Analyses). The summary of this program is given in the other work of the authors (Gabryś et al., 2021), whereas the details can be found in Rees et al. (2013). These five techniques were subsequently compared to two nonautomated subjective analyses. The first is the peak-to-peak technique that is defined by the researcher in the process of executing the BE test, hereinafter referred to as peak to peak 1. The results of the  $G_{\max}$  modulus from the RC test were also integrated into the comparison. It is noteworthy that the test procedures for these two types of tests, BE and RC, are somewhat different. The main differences include different levels of strains and different

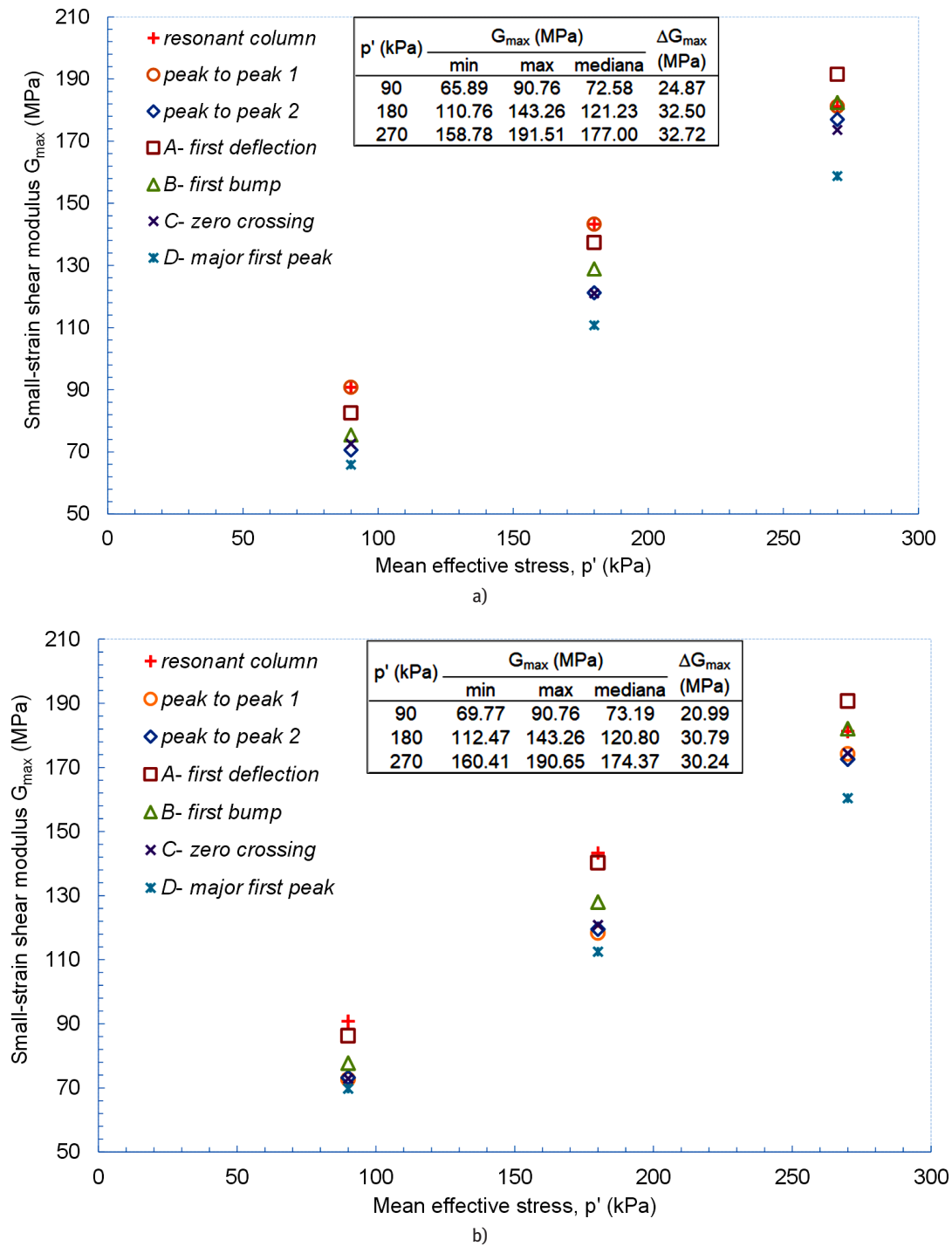


**Figure 7:** Typical plot of small-strain shear modulus ( $G_{max}$ ) against mean effective stress ( $p'$ ) from the M1 mixture: **a)**  $f_{in} = 10.0$  kHz, **b)**  $f_{in} = 12.5$  kHz.

ranges of frequencies (smaller values of both strains and resonant frequencies occur for RC tests). Despite these varieties, many researchers do not avoid comparing the small-strain stiffness results of natural soils using both techniques (Molina-Gómez et al., 2023).

As presented in Fig. 7, regardless of the excitation frequency, all procedures gave satisfactorily close values for all the tests. In this regard, it should be noted that the input signals  $f_{in} = 10.0$  and  $12.5$  kHz were the only ones repeated for each mixture and, most importantly, met the

wavelength criterion described earlier. For the input signal frequency of 10.0 kHz, the average difference between the  $G_{\max}$  results from various travel time interpretation methods was approx. 30.0 MPa, whereas for  $f_{in} = 12.5$  kHz,  $DG_{\max}$ , avg amounted to 27.3 MPa. For both frequencies offered, the lowest initial stiffness values for the RCA studied in the present research were obtained with the method *D*- major first peak. The maximum values were obtained during the RC tests (for  $p' = 90$  and 180 kPa) and with the method *A*- first deflection (for  $p' = 270$  kPa). Despite the previously mentioned differences in the BE and RC tests, the divergence between the  $G_{\max}$  results on fRCA relative to the average  $G_{\max}$  is of the order of 13%. As shown in Fig. 7, the smallest differences in the  $G_{\max}$  values (~2.0 MPa) were obtained in the case of two methods, peak to peak 2 and *C*-zero crossing, independently from the mean effective stress level. These are the results that were considered average. Then, the focus was kept only on these two signal interpretation methods. However, in assessing the travel time by the *C*-zero crossing method, difficulties were encountered in following the standard criterion because, in some of the transmissions, background noise, dispersion, and near-field effects made picking of the start of the received signal rather difficult. Given the above reasons, the peak to peak 2 technique was selected to identify the travel time to monitor the stiffness variations and, thus, the development of reaction in the fRCA blends. It was adopted for further analysis, as it provides the most consistent results for the studied anthropogenic aggregates.

By contrast, the BE tests carried out by the authors, but on natural Warsaw glacial quartz sands (Gabryś et al., 2021), have eliminated this technique, giving preference to the *C*-zero crossing and the CC procedures.

All tested fRCA compounds were analyzed in a similar way to Fig. 7, and the conclusions also apply to other mixtures.

### 3.3 Effect of an FF on $G_{\max}$

In the next order, the  $G_{\max}$  values as a function of the  $p'$  stress for all blends studied, provided by the recommended earlier method (peak to peak 2), were plotted in Fig. 8. As observed in Fig. 8, there is a clear variability and divergence in the initial stiffness of the individual mixtures, regardless of the  $f_{in}$  values. The variation in the results amounted from 20% up to almost 40%. These apparent differences are stress and FF content dependent. It seems that the preparation of the specimen (air-dry/moist conditions) is also an important factor. It can be found that for the lowest stress, the mixes of pure anthropogenic aggregates (the M1

blend, FF = 0%) were characterized by the lowest initial stiffness. This trend is confirmed reversed with increasing  $p'$ , where for  $p' = 270$  kPa, the M1 specimen had the highest stiffness. Considering only the mixtures prepared by the dry tamping method (M1 FF = 0%, M2 FF = 10%, M3 FF = 20%, M4 FF = 30%), the higher the FF content, the initially high stiffness decreased with pressure. To see if this trend of change continues, the research presented here would need to be further developed to include tests at pressures above 270 kPa and a greater number of pressures. In the case of moisturized mixtures (M5 FF = 5% and M6 FF = 15%), irrespective of  $p'$ , the lower the fines, the greater is the material shear modulus. It can be assumed that if the M1 mixture had been prepared in moist conditions, its shear modulus would have been higher than that of the M5 and M6 compounds.

The obtained experimental results are in agreement with those of other researchers, for example, He et al. (2018), dealing with the stiffness of recycled composite aggregate. They also concluded that the material with finer fractions has lower stiffness in comparison to the coarser fractions. When the soil contains a certain amount of smaller and softer (or weaker) material, the contact response is more likely to be dominated to some degree by the softest component. The surface contact behavior, in selected anthropogenic aggregates, might be changed (dropped) drastically compared to the pure fRCA, significantly reducing the wave propagation velocity and thus the mixture stiffness characteristics. In the present study, this drop in the particle contact response and, therefore, lower shear moduli only happened at higher pressures. At low pressures, the effect of the fines was not obvious.

## 4 Concluding Remarks

Regarding the studied fRCAs, as an example of anthropogenic aggregates, the following conclusions can be drawn.

- Both aspects of selecting the frequency of the test and the method of interpretation of the results appropriate for a particular anthropogenic soil are of great importance. When using the BE test method, it is crucial to be aware of all the factors that may affect the results obtained.
- In the case of fRCA mixtures, the received signal, at low input frequencies (i.e.,  $\leq 5$  kHz), was affected by the near-field effect. In contrast, at higher frequencies, approximately  $>14$  kHz, the noise levels appeared to

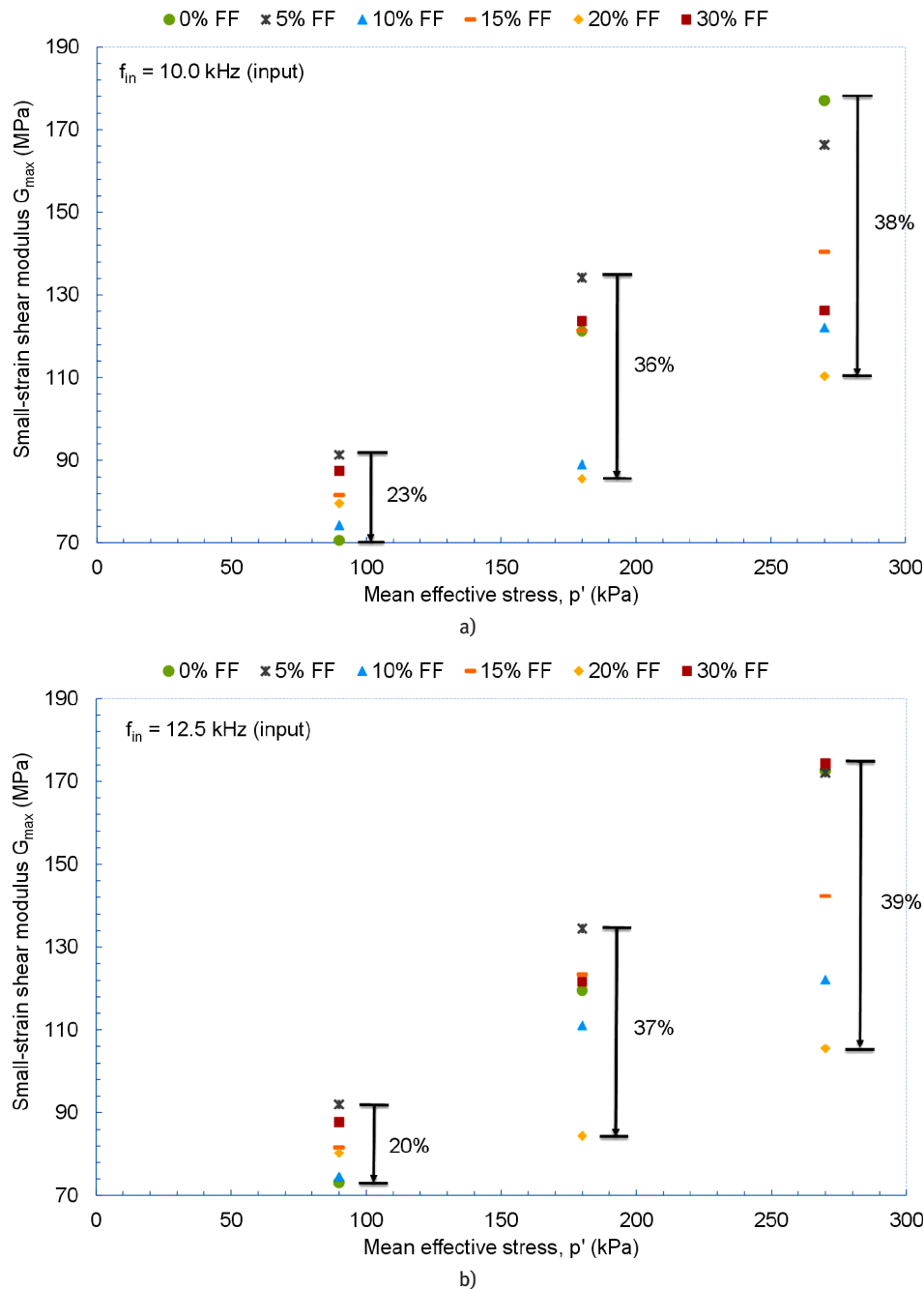


**Figure 8:** Small-strain shear modulus ( $G_{max}$ ) for fRCA mixtures based on BE test, peak to peak 2 method: a)  $f_{in} = 10.0$  kHz and b)  $f_{in} = 12.5$  kHz.

be increasing, causing some problems in determining the travel time of the S-wave. Therefore, to obtain a representative value of the small-strain shear modulus of the fRCA blend, BE measurements should be conducted at intermediate input frequencies; for this study, frequencies equal to 10.0 and 12.5 kHz were chosen.

- Concerning the differences in the travel time interpretation methods, for the selected anthropogenic aggregates, the peak-to-peak method was chosen to

identify the travel time and, consequently, estimate the initial shear modulus of the mixtures. It would be worthwhile to consider using artificial intelligence techniques in the future, for example, artificial neural network (ANN) (Hajian and Bayat, 2022), to make the selection of a technique for interpreting test results easier and more efficient. Artificial intelligence techniques are useful for predicting laboratory results without having to pay for more experiments, but a sufficient experimental dataset is required.

- The small-strain shear modulus of the fRCA compounds from the RC and BE tests was found to be in good agreement, despite differences in the test procedures themselves.
- The presence of the FF content in the studied mixtures may have softened the particle contact response, which led, especially at higher pressures, to a decrease in the initial stiffness characteristics. At a low pressure, the impact of fine particles was not evident.

## References

- [1] Arroyo, M., Muir Wood, D., and Greening, P.D. (2003). Source near-field effects and pulse tests in soil samples. *Géotechnique*. 53(3), 337–45. <http://doi.org/10.1680/geot.2003.53.3.337>.
- [2] Arulnathan, R., Boulanger, R.W. and Riemer, M.F. (1998). Analysis of bender element tests. *ASTM Geotechnical Testing J.* 21(2), 120–31. <http://doi.org/10.1520/gtj10750j>.
- [3] Basu, D., Misra, A., Puppala, A.J. and Chittoori, C.S. (2013). Sustainability in Geotechnical Engineering. In *Proceedings of the 18th International Conference on Soil Mechanics and Geotechnical Engineering*, Paris 2013. 3171–3174.
- [4] Behera, M., Bhattacharyya, S.K., Minocha, A.K., Deoliya, R. and Maiti, S. (2014). Recycled aggregate from C&D waste & its use in concrete – A breakthrough towards sustainability in construction sector: A review. *Constr Build Mater.* 68, 501–516. <http://dx.doi.org/10.1016/j.conbuildmat.2014.07.003>.
- [5] Blewett, J., Blewett, I. J., and Woodward, P. K., (2000). Phase and Amplitude Responses Associated with the Measurement of Shear-Wave Velocity in Sand by Bender Elements. *Can. Geotech. J.* 37, 1348–1357. <https://doi.org/10.1139/t00-047>.
- [6] Brignoli, E., Gotti, M., and Stokoe K.H. II (1996). Measurement of shear waves in laboratory specimens by means of piezoelectric transducers. *ASTM Geotech. Test. J.* 19 (4), 384–397.
- [7] Gabryś, K., Dołyżk-Szypcio, K., Szypcio, Z. and Sas W. (2023a). Stress–Strain Behavior of Crushed Concrete as a Special Anthropogenic Soil. *Materials*. 16(23), 7381. <https://doi.org/10.3390/ma16237381>.
- [8] Gabryś, K., Šadzevičius, R., Dapkienė, M., Ramukevičius, D. and Sas, W. (2023b). Effect of a Fine Fraction on Dynamic Properties of Recycled Concrete Aggregate as a Special Anthropogenic Soil. *Materials*. 16, 4986. <https://doi.org/10.3390/ma16144986>.
- [9] Gabryś, K., Soból, E., Sas, W., Šadzevičius, R. and Skominas, R. (2021). Warsaw glacial quartz sand with different grain-size characteristics and its shear wave velocity from various interpretation methods of BET. *Materials*. 14(3), 544. <https://www.mdpi.com/1996-1944/14/3/544>.
- [10] Gabryś, K., Sas, W., Soból, E. and Gluchowski, A. (2017). Application of Bender Elements Technique in Testing of Anthropogenic Soil—Recycled Concrete Aggregate and Its Mixture with Rubber Chips. *Appl. Sci.* 7, 741. <https://doi.org/doi:10.3390/app7070741>.
- [11] Hajian, A. and Bayat, M. (2022). Prediction of maximum shear modulus (Gmax) of granular soil using empirical, neural network and adaptive neuro fuzzy inference system models. *Geomech. Eng.* 31(3), 291–304. <https://doi.org/10.12989/gae.2022.31.3.291>.
- [12] Molina-Gómez, F., Viana da Fonseca, A., Ferreira, C. and Camacho-Tauta, J. (2023). Small- strain stiffness of liquefiable sands: a comparison between bender elements and resonant-column tests. In *Proceedings of the 8th International Symposium on Deformation Characteristic of Geomaterials*, Porto, Portugal, 3–6 September 2023. Available online. Accessed on 25 October 2023.
- [13] He, H. and Senetakis, K. (2016). A study of wave velocities and poisson ratio of recycled concrete aggregate. *Soils Found.* 56(4), 593–607. <https://doi.org/10.1016/j.sandf.2016.07.002>.
- [14] He, H., Senetakis, K. and Coop, M.R. (2018). Stiffness of a recycled composite aggregate. *Soil Dyn. Earthq. Eng.* 110, 185–194. <https://doi.org/10.1016/j.soildyn.2018.02.001>.
- [15] Hopwood, B., Mellor, M. and O'Brien, G. (2005). Sustainable Development: Mapping Different Approaches. *Sust. Dev.* 13, 38–52. <http://dx.doi.org/10.1002/sd.244>.
- [16] Ingale, R., Patel, A. and Mandal, E. (2017). Performance analysis of piezoceramic elements in soil: A review. *Sens. Actuators A: Phys.* 262, 46–63. <http://dx.doi.org/10.1016/j.sna.2017.05.025>.
- [17] Jastrzębska, M. and Łupieżowiec, M. (2023). Application of Clay–rubber Mixtures for the Transportation Geotechnics—the Numerical Analysis. *Studia Geotech. et Mech.* 45(s1), 370–381. <https://doi.org/10.2478/sgem-2023-0020>.
- [18] Jovicic, V., Coop, M.R. and Simic, M. (1996). Objective criteria for determining Gmax from bender element tests. *Géotechnique*, 46(2), 357–62. <https://doi.org/10.1680/geot.1996.46.2.357>.
- [19] Juneja, A. and Endait, M. (2013). Advances in small strain measurement using bender. In *Proc. Indian Geotech. Conf.* 1–8.
- [20] Lawrence, F.V. (1963). Propagation of ultrasonic waves through sand. *Research Report R63* 8. Cambridge, MA: Massachusetts Institute of Technology; 1963.
- [21] Lee, J.S. and Santamarina, C. (2005). Bender Elements: Performance and Signal Interpretation. *J. Geotech. Geoenviron. Eng.*, 131(9), 1063–1070. [https://doi.org/10.1061/\(ASCE\)1090-0241\(2005\)131:9\(1063\)](https://doi.org/10.1061/(ASCE)1090-0241(2005)131:9(1063)).
- [22] Lings, M. and Greening, P. (2001). A novel bender/extender element for soil testing. *Géotechnique*. 51(8), 713–7. <https://doi.org/10.1680/geot.2001.51.8.713>.
- [23] Kawaguchi, T., Mitachi, T. and Shibuya, S. (2001). Evaluation of shear wave travel time in laboratory bender element test. In *Proceedings of 15th International Conference on Soil Mechanics and Geotechnical Engineering*, Istanbul, Vol. 1, 155–158.
- [24] Makul, N., Fediuk, R., Amran, M., Zeyad, A.M., Murali, G., Vatin, N., Klyuev, S., Ozbakkaloglu, T. and Vasilev, Y. (2021). Use of Recycled Concrete Aggregates in Production of Green Cement-Based Concrete Composites: A Review. *Crystals* 11, 232. <https://doi.org/10.3390/cryst11030232>.
- [25] Markowska-Lech, K., Sas, W., Lech, M., Gabryś, K. and Szymański, A. (2018). The small strain stiffness from bender elements tests for clayey soils. *Ann. Warsaw Univ. of Life Sci. – SGGW, Land Reclam.* 50 (4), 353–371. <https://doi.org/10.2478/sggw-2018-0028>.



- [26] Mohsin, A.K.M. and Airey, D. (2003). Automating Gmax Measurements in Triaxial Tests. In *Proceedings of the 3rd International Symposium on Deformation Characteristics of Geomaterials*, IS-Lyon'03, 24 September 2003, pp.73–80.
- [27] Ogino, T. (2019). Travel time observation using numerical simulation of bender element testing in time and frequency domain. *Soils Found.* 59(3), 657–670. <https://doi.org/10.1016/j.sandf.2019.01.001>.
- [28] PN-EN ISO 14688-2:2018-05 Rozpoznanie i badania geotechniczne -- Oznaczanie i klasyfikowanie gruntów -- Część 2: Zasady klasyfikowania (In Polish) Geotechnical investigation and testing - Identification and classification of soil - Part 2: Principles for a classification.
- [29] Rees, S., Le Compte, A. and Snelling, K. (2013). A new tool for the automated travel time analyses of bender element tests. In *Proceedings of the 18th International Conference on Soil Mechanics and Geotechnical Engineering*, Paris, France, 2013; pp. 2843–2846.
- [30] Sanchez-Salinero, I., Roesset, J.M., Stokoe, K.H. and Kenneth, H. (1986). *Analytical Studies of Body Wave Propagation and Attenuation*, pp. 272.
- [31] Santamarina, J.C. and Fam, M.A. (1997). Discussion on 'Interpretation of Bender Element Tests' (paper by Viggiani and Atkinson, 1995). *Géotechnique*, 47(4), 873–877.
- [32] Sas, W., Gabryś, K., Soból, E. and Szymański, A. (2016). Dynamic Characterization of Cohesive Material Based on Wave Velocity Measurements. *Appl. Sci.* 6(2), 49. <https://doi.org/10.3390/app6020049>.
- [33] Scarrow, J. A. and Gosling, R. C. (1986). An example of rotary core drilling in soils. *Geol. Soc. Lond. Eng. Geol. Spec. Publ.* 2 (1), 357–363. <https://doi.org/10.1144/GSL.1986.002.01.60>.
- [34] Shirley, D.J. and Anderson, A.L. (1975). In situ measurement of marine sediment acoustical properties during coring in deep water. *IEEE Trans Geosci Electron*, 13(4), 163–9.
- [35] Tasalloti, A., Chiaro, G., Banasiak, L. and Palermo, A. (2020). Experimental investigation of the mechanical behaviour of gravel granulated tyre rubber mixtures. *Constr. Build. Mater.* 273, 121749. <https://doi.org/10.1016/j.conbuildmat.2020.121749>.
- [36] Viana da Fonseca, A., Ferreira, C. and Fahey, M. (2009). A Framework Interpreting Bender Element Tests, Combining Time-Domain and Frequency-Domain Methods. *Geotech. Test. J.* 32(2), 1–17.
- [37] Viggiani, G. (1995). Panelist discussion: Recent advances in the interpretation of bender element tests. In *Pre-failure Deformation of Geomaterials*. Balkema, Rotterdam, Vol. 2, 1099–1104.
- [38] Viggiani, G. and Atkinson, J. (1995). Stiffness of fine-grained soil at very small strains. *Géotechnique*, 45(2), 249–65. <https://doi.org/10.1680/geot.1995.45.2.249>.
- [39] Wang, Y.H., Lo, K.F., Yan, W.M. and Dong, X.B. (2007). Measurement biases in the Bender element test, *J. Geotech. Geoenvironmental Eng.* 133, 564–574. [http://dx.doi.org/10.1061/\(ASCE\)1090-0241\(2007\)133:5\(564\)](http://dx.doi.org/10.1061/(ASCE)1090-0241(2007)133:5(564)).
- [40] Wang, Y., Benahmed, N. and Tang A.M. (2017). A novel method for determining the small- strain shear modulus of soil using the bender elements technique. *Can Geotech J.* 54 (2), 280–9. <https://doi.org/10.1139/cgj-2016-0341>.
- [41] Wang, F., Li, D., Du, W., Zarei, C. and Liu, Y. (2021). Bender Element Measurement for Small- Strain Shear Modulus of Compacted Loess. *Int. J. Geomech.* 21(5), 04021063. [https://doi.org/10.1061/\(ASCE\)GM.1943-5622.00020](https://doi.org/10.1061/(ASCE)GM.1943-5622.00020).
- [42] Yamashita, S., Fujiwara, T., Kawaguchi, T., Mikami, T., Nakata, Y. and Shibuya, S. 2007. International Parallel Test on the Measurement of Gmax Using Bender Elements. Organized by Technical Committee 29 of the International Society for Soil Mechanics and Geotechnical Engineering ([http://www.jiban.or.jp/e/tc29/BE\\_Inter\\_PP\\_Test\\_en.pdf](http://www.jiban.or.jp/e/tc29/BE_Inter_PP_Test_en.pdf), last accessed at 5 December 2007).
- [43] Youn, J.-U., Choo, Y.-W. and Kim, D.-S. (2008). Measurement of small-strain shear modulus Gmax of dry and saturated sands by bender element, resonant column, and torsional shear tests. *Can Geotech J.* 45(10), 1426–38. <https://doi.org/10.1139/T08-069>.
- [44] Zhou, Y., Chen, Y. and Shamoto, Y. (2010). Free type bender elements for characterising soil in centrifuge model tests, *Phys. Model. Geotech.* Springman, Taylor Fr. 417, <http://dx.doi.org/10.1017/CBO9781107415324.004>.